Inorganic Chemistry

Article

pubs.acs.org/IC

Cooperatively Enhanced Ion Pair Binding with a Hybrid Receptor

Toni Mäkelä, Elina Kalenius, and Kari Rissanen*

Nanoscience Center, Department of Chemistry, University of Jyvaskyla, P.O. Box 35, FI-40014 Jyvaskyla, Finland

Supporting Information

ABSTRACT: A simple 18-crown-6-based bis-urea receptor $\mathbf{R^1}$ was synthesized in three steps from a commercial starting material. The receptor's behavior toward anions, cations, and ion pairs was studied in solution with ^{1}H NMR, in solid state with single-crystal X-ray diffraction, and in gas phase with mass spectrometry. In 4:1 $CDCl_3$/dimethyl sulfoxide solution the receptor's binding preference of halide anions is $I^- < Br^- < Cl^-$ following the trend of the hydrogen-bonding acceptor ability of the anions. The receptor shows a remarkable positive cooperativity toward halide anions Cl^-, Br^-, and I^- when complexed with Na^+, K^+, or Rb^+. The solid-state binding modes of $\mathbf{R^1}$ with alkali and ammonium halides or oxyanions were confirmed by the X-ray structures of $\mathbf{R^1}$ with KF, KCl, KBr, KI, RbCl, NH_4Cl, NH_4Br, KAcO, K_2CO_3, and K_2SO_4. They clearly present two different binding modes, either as separated or contact ion pairs depending on the nature and size of the bound cation and anion. Complexation capability of $\mathbf{R^1}$ in the gas phase was studied with competition experiments with electrospray ionization mass spectrometry showing preference of KCl complexation over NaCl, KBr, or KI supporting the results obtained in solution.

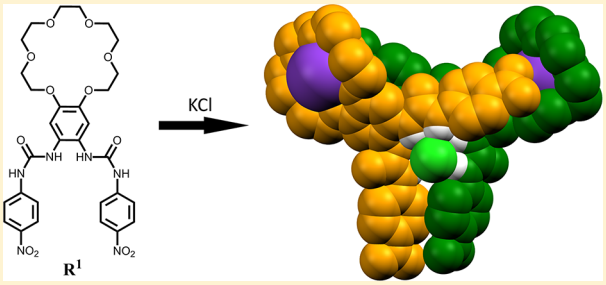

INTRODUCTION

Since the dawn of supramolecular chemistry one widely studied area in the field has been the development of synthetic receptors toward cations and anions.[1] Possibly due to the more simple interactions with cations, the development of cation receptors has been a more extensively studied area of supramolecular chemistry. Only recently the anion receptor chemistry and the research of anion recognition has leveled with the cation receptor development. Crown ethers have been thoroughly studied since their discovery by Pedersen in 1967,[2,3] and they have been utilized in various receptors as cation binding subunits.[4] Anions have huge importance in nature and in living organisms, which explains the ever-growing interest and need to develop more effective and sophisticated anion receptors. This in spite of the complications anion recognition has due to the higher solvation energies and more complicated geometries of anions.[1] Various anion binding functionalities, such as urea, thiourea, amide, squaramide, amine or ammonium, pyrrole, and indole moieties, and generally Lewis acids, have been incorporated to different types of molecular scaffolds to develop stronger and more specific anion receptors that interact with the guest through various weak interactions.[5−10] Although a lot of effort has been focused on the development of ion receptors capable of binding either anion or cation, the development of ditopic ion pair receptors has attracted a growing interest during the last two decades.[11−14] From the studies focused on single ion receptors it has become clear that the ability of receptor to bind simultaneously both cation and anion could lead to more selective and effective receptors. Studying ion pair recognition has more complications compared to the single ion binding receptors due to the various ion pair interaction equilibriums, which might be present in the system, and the energetic costs of separating the ions.[15−17] Because of this ion pair receptors must be designed to overcome this energetic cost, which, in turn, might lead to difficult synthesis of structurally complicated host molecules. Recent reviews of ditopic receptors present a variety of different molecular architectures combined with well-known recognition functionalities for cations and anions. These ion pair receptors show more efficient binding of the desired guest (either cation or anion) and thus have been used in many applications, such as ion transport through lipid membranes, salt solubilization, sensors, or logic gates.[11−14] Contemporary highlights are examples where ion pair receptors bind three[18,19] or even four guests simultaneously.[20]

Smith et al.,[21] Barboiu et al.,[22,23] and Nam et al.[24] have studied the combined use of a crown ether and urea functionalities for simultaneous cation and anion binding. The combination of simple, yet effective structural elements also gives possibilities to develop receptor scaffolds with different spatial arrangements of well-known cation and anion recognition sites. Some recent work by Romanski et al.[25] and Albrecht et al.[26] present examples of using L-ornithine moiety jointly with an aza-crown ether or a quinoline benzocrown to boost the anion recognition abilities of the receptors through positive cooperative effects induced by cation binding. Jeong et al.[27] have also prepared an aza-crown derivative capable of transporting inorganic salts through phospholipid membranes

Received: July 15, 2015
Published: September 3, 2015

DOI: 10.1021/acs.inorgchem.5b01577
Inorg. Chem. 2015, 54, 9154−9165

Scheme 1. Syntheses of Receptors[a,b] R^1 and R^2 and Single-Crystal X-ray Structures of 2, 3, and R^1

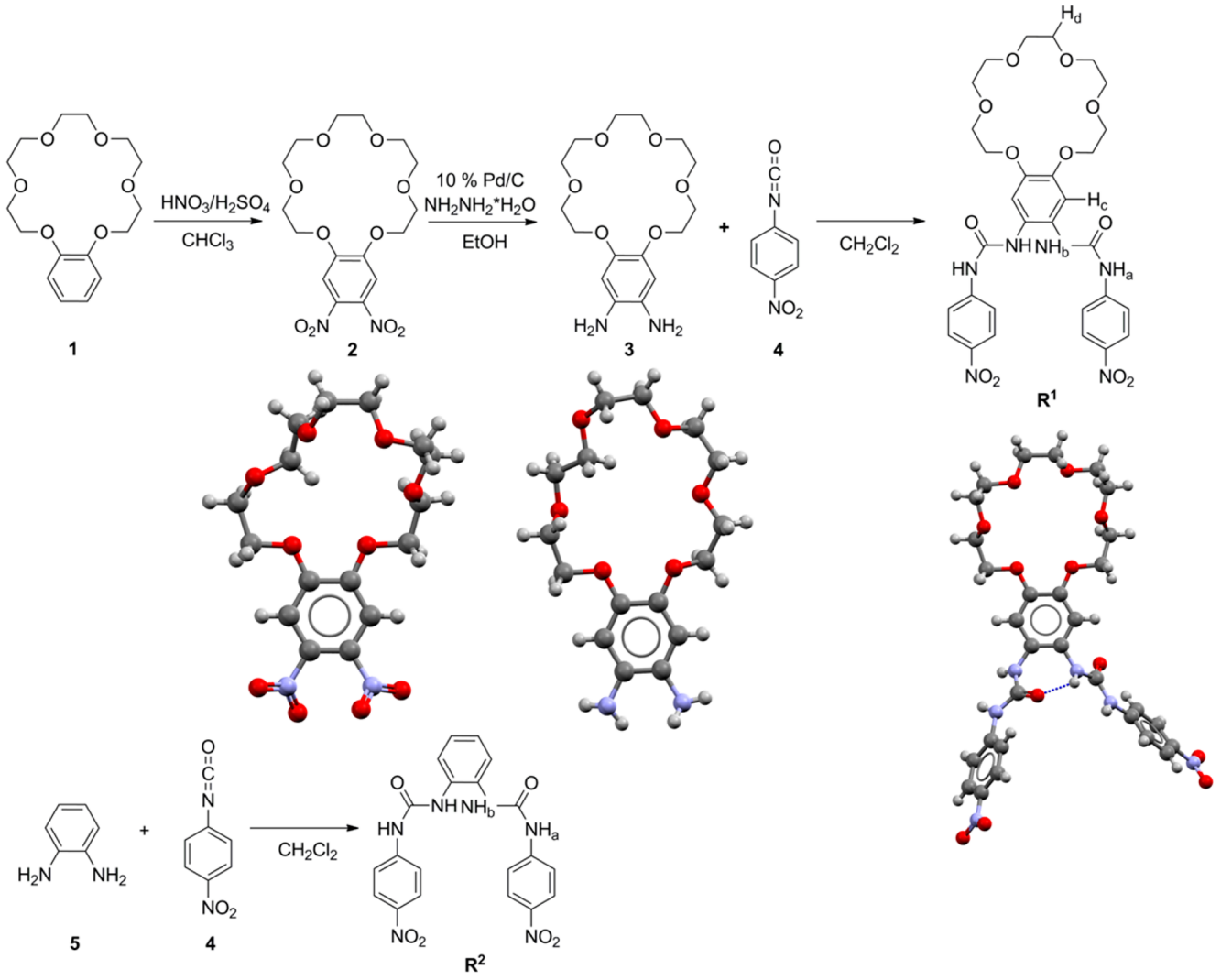

[a]The protons H_a, H_b, H_c and H_d monitored during solution studies are given in the structural formulas of R^1 and H_a, H_b in R^2. [b]Solvent molecules and disorder is omitted from the crystal structure pictures.

showing positive cooperative effects for ion pair binding and selectivity for certain ion pairs depending on the aza-crown size.

In this work we present the anion, cation, and ion pair recognition studies of a hybrid crown ether bis-urea receptor R^1 (Scheme 1) in solution, by ^{1}H NMR titrations, and in gas phase, by mass spectrometry, via competition experiments. The electrospray ionization mass spectrometry (ESI-MS) studies support the ion pair binding preferences observed in solution. The ion pair recognition of R^1 in the solid state has been extensively studied by single-crystal X-ray diffraction for 10 different cation−anion pairs. In addition to the solid-state structures of the halide complexes studied in solution and in gas phase also X-ray structures of a set of oxyanion complexes are reported revealing the versatile binding nature of the receptor R^1.

RESULTS AND DISCUSSION

Synthesis and Characterization. The receptor R^1 was prepared by a three-step synthesis starting from a commercially available benzo-18-crown-6 compound **1** (Scheme 1). The starting material was nitrated by a two-phase reaction in chloroform and nitric acid/sulfuric acid mixture.[28] The dinitro product **2** was obtained in 77% yield. Compound **2** was reduced to the diamine **3** with hydrazine monohydrate and 10% palladium on activated charcoal in argon atmosphere.[28] The diamine **3** was obtained in >95% yield and used without further purification in the subsequent condensation reaction with 4-nitrophenylisocyanate under argon atmosphere resulting in the desired receptor R^1, which precipitated from the reaction mixture as yellow solid (see Supporting Information for details). R^1 was recrystallized by a slow diffusion of methanol into dimethylformamide (DMF) solution and was obtained in 52% yield. The receptor R^1 had a fairly limited solubility in most organic solvents, but it was well-soluble in polar solvents like dimethyl sulfoxide (DMSO) and DMF. The reference receptor R^2 without the crown ether moiety is a known compound and was synthesized according to the literature method[29] using dichloromethane as solvent. R^2 precipitated from the reaction mixture and was used without further purification. Both receptors were analyzed by ^{1}H and ^{13}C NMR and ESI-MS, and R^1 was analyzed with single-crystal X-ray analysis. The diamine **3** was characterized by ^{1}H NMR and

DOI: 10.1021/acs.inorgchem.5b01577
Inorg. Chem. 2015, 54, 9154−9165

single-crystal X-ray analysis (see Scheme 1 and Supporting Information).

Solution Studies. Solution complexation studies were performed to study the affinity of $\mathbf{R^1}$ toward alkali metal cations and halide anions and to probe if $[\mathbf{R^1}\cdot\text{cation}]^+$ complex has enhanced affinity toward halide anions compared to the alkali metal-free $\mathbf{R^1}$ alone. The preliminary studies done in noncompetitive 9:1 $CDCl_3$/DMSO mixture showed very strong binding between $[\mathbf{R^1}\cdot\text{cation}]^+$ complex and chloride (log K > 5). Therefore, more competitive 4:1 $CDCl_3$/DMSO solvent system was chosen to reduce the binding and to have more reliable binding constants. The studies were started with Job plot experiments (see Figures S6–S9) and continued as ^{1}H NMR titrations in 4:1 $CDCl_3$/DMSO (anion and ion pair studies) and, due to solubility reasons of $MBPh_4$, in pure DMSO (cation binding studies). Test experiment was performed with $TBABPh_4$ to rule out the interaction of these ions with $\mathbf{R^1}$ (Figure S33). The reference receptor $\mathbf{R^2}$ was used only for anion binding studies and to probe if the presence of cation interferes with the anion recognition ability of $\mathbf{R^2}$. All binding constants (log K) were calculated with HypNMR2008[30] using global analysis[31] (i.e., using multiple proton resonances simultaneously for the calculation), applying 1:1 binding model for the anion and some ion pair titrations. For cation titrations 1:2 binding model and for a few ion pair titrations also 2:1 binding model was used (details are presented further in the text and in the Supporting Information).

Cation Binding Studies. The affinity of $\mathbf{R^1}$ toward alkali metal cations was studied for Na^+, K^+, Rb^+, and Cs^+ in DMSO. The cations were used as their tetraphenylborate (BPh_4^-) salts. The large counteranion was used due to its inert hydrogen bonding nature in the anion binding. The chemical shift changes of protons H_c and H_d (see Scheme 1 for proton assignment) were followed during the titration experiments (Figure 1). The aromatic protons H_c showed a steady

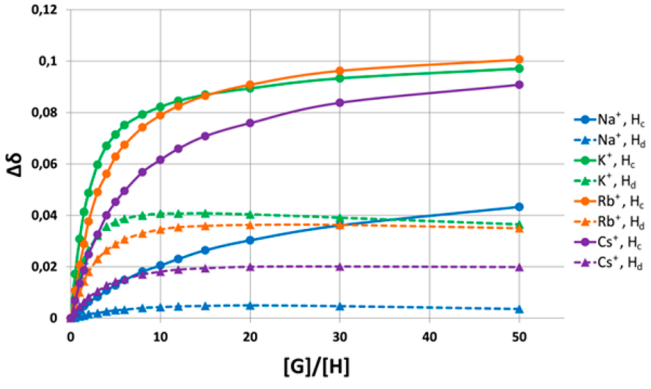

Figure 1. Chemical shift changes for protons H_c (solid line) and H_d (dashed line) upon titrating $\mathbf{R^1}$ with Na^+ (blue), K^+ (green), Rb^+ (orange), and Cs^+ (purple) alkali metal cations as their BPh_4^- salts in DMSO.

downfield shift for all the studied cations with maximum shifts of 0.043, 0.097, 0.101, and 0.091 ppm for Na^+, K^+, Rb^+, and Cs^+, respectively (50 equiv of the guest). The chemical shift change of aromatic H_c protons show a typical behavior for 1:1 binding stoichiometry, but interestingly the crown ether protons H_d undergo first a downfield shift upon increasing cation concentrations. With very high guest concentrations, however, H_d starts to move upfield. With potassium cation the upfield shift starts to become apparent after 10 equiv; with other cations downfield shift is prominent up to 20 equiv, after which the proton starts to show upfield shift (Figure 1). After 10 equiv of guest addition the CH_2 protons (H_d) of the crown ether show 0.041 ppm downfield shift in the case of K^+, and with Na^+, Rb^+, and Cs^+ the chemical shift changes for 10 equiv additions are 0.0043, 0.035, and 0.018 ppm, respectively. With the maximum cation addition (50 equiv) the chemical shift change of H_d in the case of K^+ is 0.037 ppm, and for Na^+, Rb^+, and Cs^+ the chemical shift changes are 0.0036, 0.035, and 0.020 ppm. Binding behavior of $\mathbf{R^1}$ was modeled with 1:2 binding stoichiometry with HypNMR2008[30] although the Job plot analysis shows clearly 1:1 binding stoichiometry for K^+ (see Figure S6). The problem using Job plot analysis to confirm the binding stoichiometry in complex systems has been brought up by Thordarson.[31] Because of the large excess (50 equiv) of the cation guest added to the solution the binding can be modeled in more complex stoichiometry, which might not be in agreement with Job plot analysis.

As can be seen from the binding constants (Table 1), the potassium has clearly the strongest binding affinity for $\mathbf{R^1}$ with

Table 1. Binding Constants[a] (log K) Obtained from Cation and Anion Titrations for Receptors $\mathbf{R^1}$ and $\mathbf{R^2}$

		$\mathbf{R^1}$	$\mathbf{R^2}$
$\mathbf{Na^+}$ [b]	log K_{11} [c]	1.52(3)	
	log K_{12} [c]	0.02(8)	
$\mathbf{K^+}$ [b]	log K_{11}	2.51(1)	
	log K_{12}	0.65(30)	
$\mathbf{Rb^+}$ [b]	log K_{11}	2.18(2)	
	log K_{12}	0.97(47)	
$\mathbf{Cs^+}$ [b]	log K_{11}	1.98(3)	
	log K_{12}	0.80(47)	
$\mathbf{Cl^-}$ [d]	log K_{11}	2.87(6)	2.91(1)
$\mathbf{Br^-}$ [d]	log K_{11}	2.21(1)	2.42(1)
$\mathbf{I^-}$ [d]	log K_{11}	1.53(3)	1.43(2)

[a]The fitting error of the binding constant is given in parentheses. [b]Performed in DMSO. [c]The numbering denotes the stoichiometry of the complexation; K_{xy}, where x = host, y = guest. [d]Performed in 4:1 $CDCl_3$/DMSO.

log K_{11} value of 2.51. This is not surprising due to the good size match between potassium cation and 18-crown-6. The cation binding affinity of $\mathbf{R^1}$ is reduced with the larger cations because of the size mismatch and the stronger polarizability of the larger cations. The log K_{11} values are 2.18 for Rb^+ and 1.98 for Cs^+, but the binding affinity for Na^+ is surprisingly low (log K_{11} = 1.52). This probably is resulting from the strong solvation of the sodium cation in highly polar DMSO solvent. The binding of the second cation can be rationalized by additional interactions with the noncrown ether parts of the receptor molecule at very high guest concentrations. However, this second binding is very weak (Table 1). The clear non-cooperativity of the second binding event can easily be explained because of the electrostatic repulsions between the cationic guests. All the details for binding constant calculations and the binding isotherms can be found in the Supporting Information (Figures S10–S13).

Anion Binding Studies. Halide anion (Cl^-, Br^-, I^-) binding affinities of $\mathbf{R^1}$ and $\mathbf{R^2}$ were studied in fairly nonpolar 4:1 $CDCl_3$/DMSO solvent mixture. Titrations were performed up

DOI: 10.1021/acs.inorgchem.5b01577
Inorg. Chem. 2015, 54, 9154–9165

to 10 equiv of the anion added as their tetrabutylammonium (TBA^+) salts to rule out the possible interaction of the cation with the crown ether moiety of $\mathbf{R^1}$. In the anion titrations three different proton signals in $\mathbf{R^1}$ were followed (H_a, H_b, and H_c; see Scheme 1 for proton assignments), all of which have a similar behavior upon anion additions (Figure 2). When

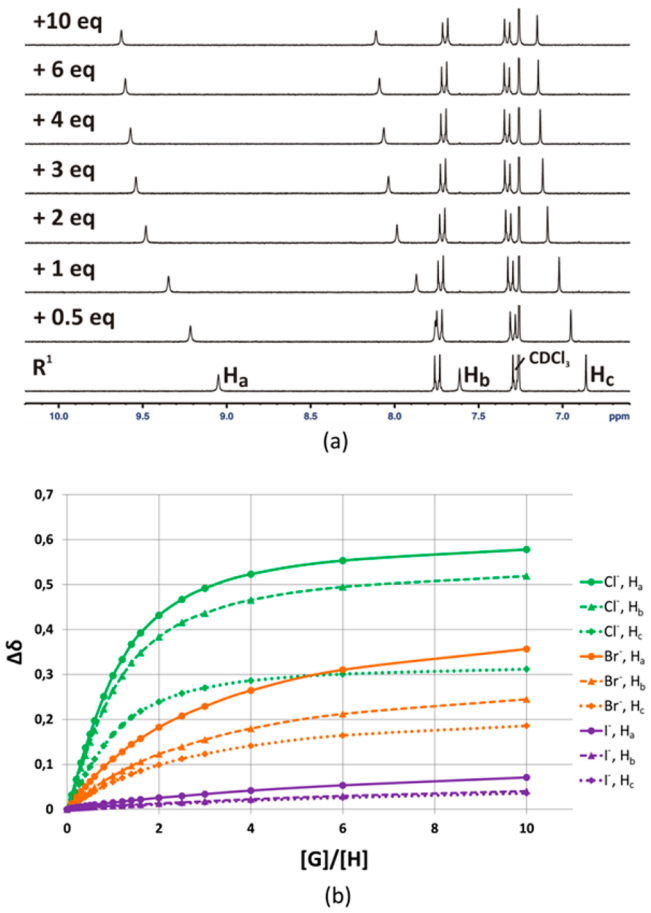

Figure 2. (a) Aromatic area of the $\mathbf{R^1}$ spectra for $\mathbf{R^1}$ + TBACl– titration. Only selected spectra are presented. The protons H_a, H_b, and H_c that undergo significant chemical shift changes upon chloride addition are named in the spectra. (b) The chemical shift change for H_a (solid line), H_b (dashed line), and H_c (dotted line) for Cl^- (green), Br^- (orange), and I^- (purple) titrations.

titrating $\mathbf{R^1}$ with Cl^- the urea protons H_a and H_b show a downfield shift of 0.58 and 0.52 ppm, respectively, upon formation of $\mathbf{R^1}\cdot Cl^-$ complex through hydrogen bonding interactions (Figure 2a). Interestingly, also aromatic protons H_c undergo a similar downfield shift of 0.31 ppm (Figure 2a). This is likely due to the internal C–H···O hydrogen bonding between H_c and carbonyl oxygens of the urea groups as receptor arms can undergo a conformational change upon anion binding. The protons H_a, H_b, and H_c show similar behavior with TBABr and TBAI additions, even though the chemical shift changes are smaller than with Cl^- (Figure 2b). In the case of TBABr the urea proton H_a undergoes a downfield shift of 0.36 ppm, and the other urea proton H_b has a chemical shift change of 0.24 ppm when 10 equiv of TBABr is added to the sample. The aromatic proton H_c also shows similar downfield shift behavior with chemical shift change of 0.19 ppm with maximum Br^- addition (Figure 2b). In the case of TBAI the chemical shift changes of protons H_a, H_b, and H_c are 0.07, 0.04, and 0.04 ppm, respectively, being remarkably smaller when compared to Cl^- and Br^- induced changes. This is understandable due to the weaker hydrogen bond acceptor character of iodide (Figure 2b).

The anion binding constants were calculated using 1:1 binding model (Table 1) supported by the Job plot analysis (Figure S7). The binding affinity of $\mathbf{R^1}$ toward the halide anions has a clear trend with the Lewis basicity of the anions. The $\mathbf{R^1}\cdot Cl^-$ complex has log K_{11} value of ~2.87, while $\mathbf{R^1}\cdot Br^-$ and $\mathbf{R^1}\cdot I^-$ complexes have log K_{11} values of 2.21 and 1.53, respectively. Not surprisingly the reference receptor $\mathbf{R^2}$ has very similar binding affinity for the halides with log K_{11} values of ~2.91, 2.42, and 1.43 for Cl^-, Br^-, and I^-, respectively. These results suggest that the crown ether moiety does not have a large effect on the anion binding behavior of the urea part of the receptor and that the urea protons have similar hydrogen bonding abilities in both $\mathbf{R^1}$ and $\mathbf{R^2}$. All the details concerning the anion titrations can be found in the Supporting Information (Figures S14–S19).

Ion Pair Binding. Ion pair titrations were performed in the same solvent mixture as the anion binding studies (4:1 $CDCl_3$/DMSO). The receptor $\mathbf{R^1}$ and 1 equiv of the chosen cation as its BPh_4^- salt were dissolved in the solvent mixture. The titration of resulting $\mathbf{R^1}\cdot cation^+$ complex with halide anions (Cl^-, Br^-, I^-) as their TBA^+ salts resulted in similar downfield shifts of $\mathbf{R^1}$ protons H_a, H_b, and H_c as without the presence of an alkali metal cation, although the changes were more drastic in the presence of a cation (Figure 3a,b). During the titration of $\mathbf{R^1}\cdot K^+$ complex with TBACl, the urea proton H_a undergoes a downfield shift of 0.61 ppm being only slightly larger than the chemical shift change of H_a when only $\mathbf{R^1}$ and Cl^- were used (0.58 ppm). More surprisingly the urea proton H_b of $\mathbf{R^1}\cdot K^+$ complex shows a total chemical shift change of 0.62 ppm after 10 equiv addition of TBACl, which is considerably larger than for titration with $\mathbf{R^1}$ alone (0.52 ppm), indicating stronger hydrogen bonding interactions between H_b and Cl^- when cation is bound to the crown ether unit (Figure 3b). Finally, the aromatic proton H_c in $\mathbf{R^1}\cdot K^+$ complex shows a similar behavior upon chloride binding as with $\mathbf{R^1}$ alone with a chemical shift change 0.33 ppm. The protons H_a, H_b, and H_c all show clearly a plateau after addition of 2 equiv of TBACl. This is not observed for $\mathbf{R^1}$ with TBACl indicating stronger chloride binding with $\mathbf{R^1}\cdot K^+$ complex compared to $\mathbf{R^1}$ (Figure 3c). Similar observations were made also for $\mathbf{R^1}\cdot K^+$ complex in the titrations with TBABr and TBAI (Figure 3b). Upon addition of 10 equiv of TBABr, the protons H_a, H_b, and H_c undergo 0.43, 0.36, and 0.24 ppm downfield shifts, respectively, which are larger than for $\mathbf{R^1}\cdot Br^-$ complex indicating again stronger hydrogen bonding interactions between $\mathbf{R^1}\cdot K^+$ complex and Br^-. The corresponding chemical shift changes in the case of TBAI were 0.14, 0.13, and 0.09 ppm for H_a, H_b, and H_c, respectively, again showing similar trend of stronger hydrogen bonding interactions between $\mathbf{R^1}\cdot K^+$ complex and I^- (Figure 3b).

The Table 2 presents the log K values obtained by fitting the titration data into 1:1 or 2:1 binding models for the ion pair titrations (verified by Job plot analysis, Figure S8). The binding constant calculations for the $\mathbf{R^1}\cdot K^+\cdot Cl^-$ complex gave log K_{11} value of 3.95, which is remarkably higher than the binding constant for $\mathbf{R^1}\cdot Cl^-$ complex formation (log K_{11} = 2.87) alone. This is clearly evident from the chemical shift changes during the titration (Figure 3c). The binding constant for $\mathbf{R^1}\cdot K^+\cdot Br^-$ complex is 3.25, again showing a remarkable positive cooperativity for anion binding when cation is bound to the

DOI: 10.1021/acs.inorgchem.5b01577
Inorg. Chem. 2015, 54, 9154–9165

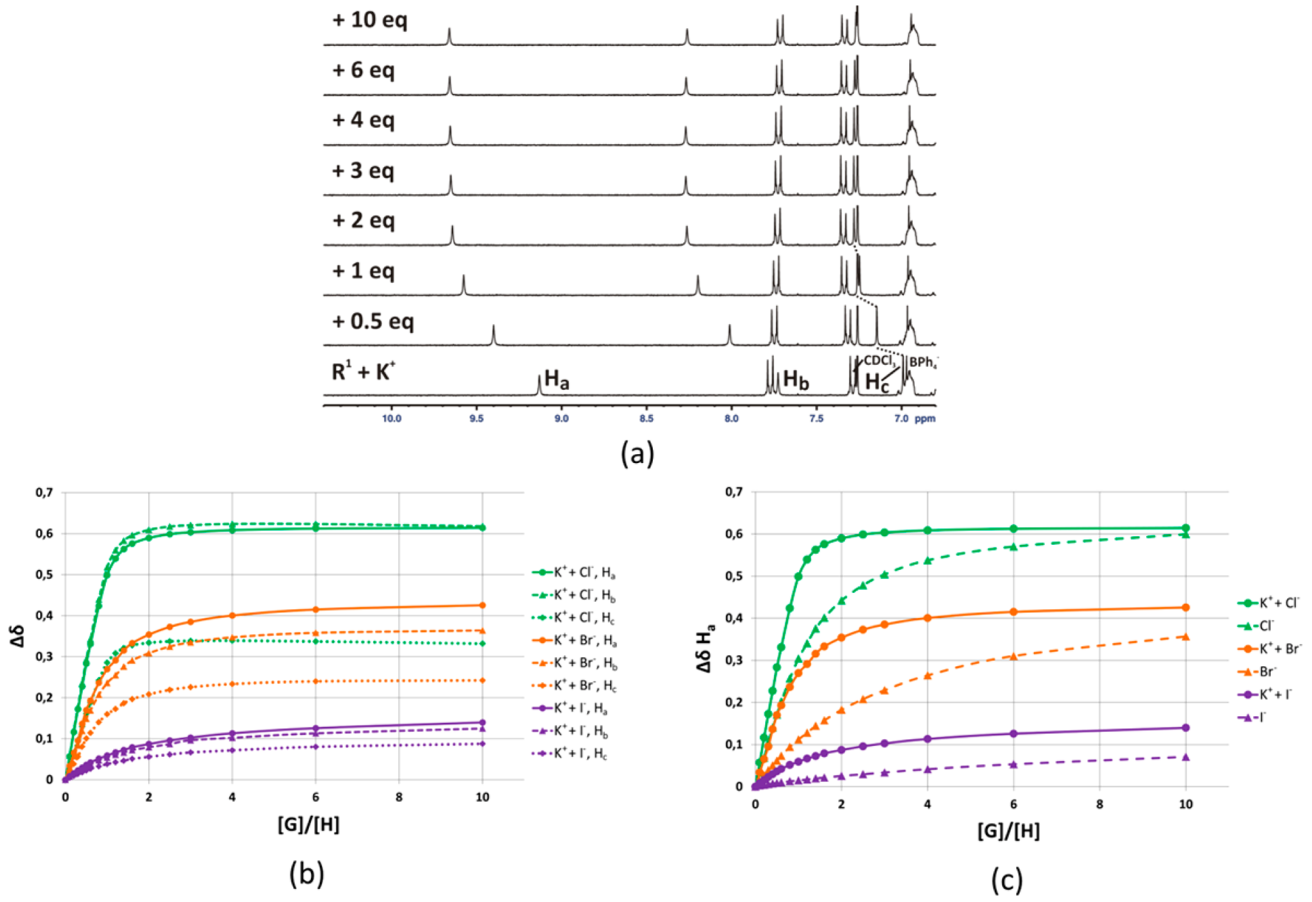

Figure 3. (a) Aromatic area of the $\mathbf{R^1}$ spectra for $\mathbf{R^1}$ + 1 equiv $KBPh_4$ + TBACl titration. Only selected spectra are presented. The protons H_a, H_b, and H_c that undergo significant chemical shift changes upon chloride addition are named in the spectra. (b) The chemical shift change differences for H_a (solid line), H_b (dashed line), and H_c (dotted line) for Cl^- (green), Br^- (orange), and I^- (purple) titrations in the presence of 1 equiv of $KBPh_4$. (c) The chemical shift change differences for H_a in titrations with Cl^- (green), Br^- (orange), and I^- (violet) without cation (dashed line) and in the presence of 1 equiv of $KBPh_4$ (solid line).

Table 2. Binding Constants[a] (log *K*) Obtained from Ion Pair Titrations for $\mathbf{R^1}$·Cation Complex with Different Halide Anions in 4:1 $CDCl_3$/DMSO

		$\mathbf{R^1}$ + Na^+	$\mathbf{R^1}$ + K^+	$\mathbf{R^1}$ + Rb^+
Cl^-	log K_{11}[c,d]	3.73(3)	3.95(1)	3.83(2)
Br^-	log K_{11}[d]	3.25(1)	3.19(8)	3.27(1)
	log K_{11}[e]	3.33(1)	3.33(4)	*b*
	log K_{21}[e]	2.38(2)	2.27(35)	*b*
I^-	log K_{11}[d]	2.61(2)	2.57(1)	2.52(2)
	log K_{11}[e]	*b*	2.67(7)	2.61(1)
	log K_{21}[e]	*b*	2.60(27)	2.69(33)

[a]The fitting error of the binding constant is given in parentheses. [b]2:1 binding model was not applicable. [c]The numbering denotes the stoichiometry of the complexation; K_{xy}, where x = host, y = guest. [d]1:1 binding model was used. [e]2:1 binding model was used.

crown ether. Similar enhancement is clearly observed with $\mathbf{R^1}$·K^+·I^- complex formation with log K_{11} value of 2.57. When $\mathbf{R^1}$·K^+·I^- complex formation was studied with Job plot analysis the results gave an indication of a more complex stoichiometry being present in the solution (see Figure S8). In the Job plot analysis chemical shift changes of H_a shows 1:1 complex stoichiometry, but the chemical shift changes of H_b and H_c indicate possible 2:1 complex. This more complex stoichiometry could be modeled with HypNMR2008[30] with 2:1 binding model for the $\mathbf{R^1}$·K^+·I^- and $\mathbf{R^1}$·Rb^+·I^- complexes resulting in a better fit between the observed and calculated chemical shift changes. For reasons unknown the binding constant could not be calculated with this binding stoichiometry for the $\mathbf{R^1}$·Na^+·I^- complex although the chemical shift changes were similar to the above-mentioned complexes. The 2:1 binding model could be applied to the $\mathbf{R^1}$·Na^+·Br^- and $\mathbf{R^1}$·K^+·Br^- complexations too, although Job plot analysis gave quite clear evidence of 1:1 binding stoichiometry (Figure S8). Using 2:1 binding model did result in slightly higher log K_{11} values for all the complexations when compared to the log K_{11} values obtained from the simple 1:1 model. The use of 2:1 binding model also gave better fit between the observed and calculated chemical shift changes (see Figures S22, S26, S28, and S32). The second binding event seems to be more dominant when the simple 1:1 complex formation is weaker as can be seen from the log K_{21} values presented in Table 2. This observation was supported by the unsuccessful application of 2:1 model for $\mathbf{R^1}$·cation·Cl^- complex where the 1:1 complexation is very strong. Detailed titration data and binding isotherms can be found in the Supporting Information (Figures S20−S32).

Surprisingly the choice of bound cation does not seem to have a noticeable effect on the anion binding affinity as evidenced by the binding constants presented in Table 2. The reason for the enhanced binding could be explained by the electrostatic interactions and the enhanced acidity of the urea

DOI: 10.1021/acs.inorgchem.5b01577
Inorg. Chem. 2015, 54, 9154−9165

hydrogens induced by the cation complexation. This is supported by the larger H_b chemical shift changes (compared to H_a chemical shift changes, Figure 3b) in the case of chloride binding with $\mathbf{R^1}$·cation$^+$ complex. One affecting factor could be also the second ion pair formation between the "naked" TBA^+ and BPh_4^- ions and its effect on the formation of $\mathbf{R^1}$·cation·halide complex. However, this was not taken into consideration when calculating the binding affinities.

To test if the observed anion recognition of the $\mathbf{R^1}$·cation complex is truly induced by the cation complexation in the crown ether part, the reference receptor $\mathbf{R^2}$ with 1 equiv of $KBPh_4$ was titrated with TBACl in 4:1 $CDCl_3$/DMSO mixture. Stepwise addition of TBACl into 2.5 mM sample of $\mathbf{R^2}$·cation mixture resulted in very small chemical shift changes in the urea protons H_a and H_b until ~0.6 equiv of Cl^- was added (Figure 4). After 1 equiv of TBACl, urea protons started to show

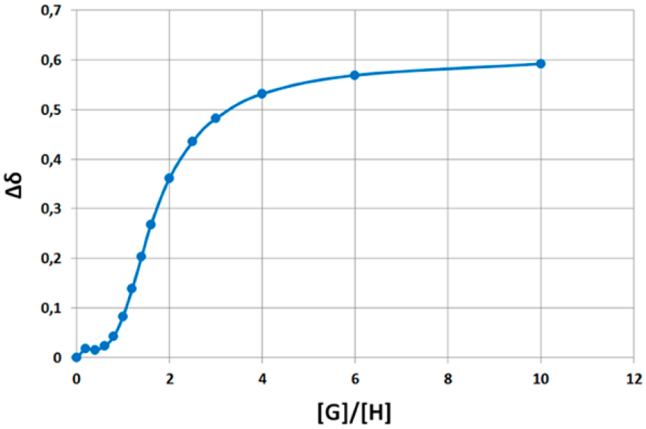

Figure 4. Chemical shift changes of H_a in $\mathbf{R^2}$ in titration of 2.5 mM $\mathbf{R^2}$ + 1 equiv of $KBPh_4$ with TBACl in 4:1 $CDCl_3$/DMSO. Some points from the beginning of the titration curve were omitted for clarity.

similar behavior to the titration of $\mathbf{R^1}$ or $\mathbf{R^2}$ alone with TBACl. This can be explained by formation of KCl ion pair in the fairly nonpolar organic solvent. This prevents the hydrogen bonding between $\mathbf{R^2}$ and Cl^- until equimolar amount of Cl^- to K^+ has been added. The excess chloride is then "free" to interact with $\mathbf{R^2}$, and the behavior is similar to 1:1 complex formation. This kind of phenomenon has been observed also by Smith,[32] and they explained that the ion pair formation between the metal cation and the anion can reduce the anion basicity and affect the receptor−anion interactions either by inducing sterical hindrance or by lowering the effective charge of the anion. This result strongly suggests that the complexation of the cation in the crown ether is responsible for the higher anion affinity of the $\mathbf{R^1}$·cation complex when compared to cation-free $\mathbf{R^1}$ or $\mathbf{R^2}$.

Solid-State Complexation. *R^1·KCl*. Solid-state complex of $\mathbf{R^1}$**·KCl** was crystallized by slow diffusion of Et_2O into CH_3OH solution of $\mathbf{R^1}$ with excess of KCl added in aqueous solution. The complexation of the salt was clearly observed by the better solubility of the complex in CH_3OH compared to the receptor $\mathbf{R^1}$ alone.

The complex crystallized in monoclinic space group $P2_1/n$ with two receptor molecules in the asymmetric unit forming a dimer with 2 equiv of KCl (Figure 5a).

In the complex $\mathbf{R^1}$**·KCl** potassium K1 has eight-coordination, while the potassium K2 has seven-coordination. Potassium K1 is bound inside the crown ether by six coordinative bonds [K1···O(crown ether) distance 2.662(2)−2.838(2) Å], and its

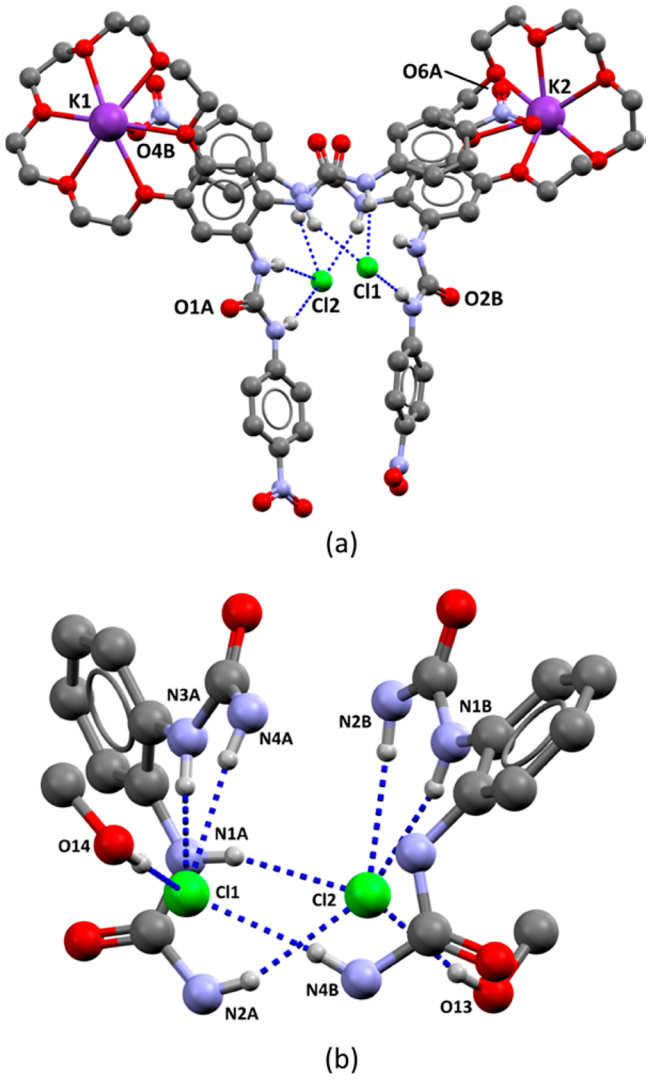

Figure 5. X-ray structure of $\mathbf{R^1}$**·KCl**. (a) Two receptor molecules form a dimer by coordination between K1 and O4B. Hydrogen bonds presented as dashed lines. Methanol molecules are omitted from the picture. (b) Dimerization leads to the formation of a urea proton-coated binding pocket for two chlorides. Similar type of solid-state complex was obtained also with KF and KBr (see Supporting Information). Disordered components in one crown ether moiety and all the nonbonding hydrogen atoms were omitted for clarity.

coordination sphere is completed by a coordinative bond [2.736(2) Å] from the nitro group's oxygen atom O4B of the other molecule of the dimer and another bond from the carbonyl oxygen O2B′ (0.5 + x, 1.5 − y, −0.5 + z) from the adjacent dimer with K1···O2B′ distance of 2.650(2) Å (Figure 5a). Potassium K2 is bound by the crown ether [K2···O(crown ether) distance 2.686(2)−2.786(2) Å] but has a slightly different coordination sphere compared to the potassium K1. The seventh coordinative bond to K2 is formed from the carbonyl oxygen O1A″ (−0.5 + x, 1.5 − y, 0.5 + z) of the adjacent dimer with K2···O1A″ distance 2.650(2) Å. There is also a very weak contact along the eight-coordination site of K2 to the nitro group oxygen O6A with a distance of 3.716(3) Å. The coordination between the potassium cations and carbonyl and nitro group oxygens leads to the formation of a one-dimensional (1D) coordination polymer along crystallographic c-axis.

DOI: 10.1021/acs.inorgchem.5b01577
Inorg. Chem. 2015, 54, 9154−9165

The dimerization forms a binding pocket decorated by eight urea protons where two chloride anions are bound by hydrogen bonds to the urea groups and methanol molecules (Figure 5b). Chloride Cl1 is bound by two hydrogen bonds to receptor A [N3A···Cl1 distance 3.311(2) Å, N3A−H···Cl1 angle 156°; N4A···Cl1 distance 3.164(2) Å, N4A−H···Cl1 angle 164°] and with one H-bond to receptor B [N4B···Cl1 distance 3.240(2) Å, N4B−H···Cl1 angle 173°]. Cl1 forms fourth hydrogen bond to a methanol molecule with O14···Cl1 distance of 3.177(2) Å (O14−H···Cl1 angle 160°). Cl2 forms two H-bonds to receptor A [N1A···Cl2 distance 3.217(2) Å, N1A−H···Cl2 angle 162°; N2A···Cl2 distance 3.292(2) Å, N2A−H···Cl2 angle 159°] and two H-bonds to receptor B [N1B···Cl2 distance 3.207(2) Å, N1B−H···Cl2 angle 164°; N2B···Cl2 distance 3.295(2) Å, N2B−H···Cl2 angle 155°]. Also Cl2 forms a hydrogen bond to another methanol molecule with O13···Cl2 distance of 3.180(2) Å (O13−H···Cl2 angle 170°).

Similar binding motif was also observed for complexes **R¹·KBr_1** (different structures with KBr indicated by numbers) and **R¹·KF** (Figures S34 and S35). It can be considered as a general solid-state binding motif for receptor **R¹** when cation size is suitable for the crown ether and counteranion has strong Lewis basicity. Bromide seems to be basic enough to have two different binding motifs in the solid state.

R¹·KBr_2. Complex **R¹·KBr_2** crystallized by slow diffusion of Et_2O into acetone solution of **R¹** with excess KBr added in aqueous solution. The addition of the guest resulted again in better solubility of the complex in acetone compared to the receptor alone. The complex crystallized in monoclinic space group $P2_1/c$ with one molecule of **R¹** and 1 equiv of KBr in the structure (Figure 6a). Interestingly, similar complex was obtained by slow diffusion of Et_2O into CH_3OH solution of **R¹** with KBr. In this case **R¹** crystallized in two different crystal forms in the same crystallization experiment, one form being isostructural to the **R¹·KCl** complex (Figure 5a and Figure S35) and the other being isostructural to the complex obtained from acetone/Et_2O crystallization experiment.

In this structure potassium K1 has eight-coordination, and it is bound to the crown ether with six bonds [K1···O(crown ether) 2.780(3)−2.967(3) Å; Figure 6b]. Although the size match between potassium and 18-crown-6 is ideal the potassium K1 is located slightly above the plane of the crown ether. The seventh coordinative bond to K1 is a contact ion pair with Br1 (K1···Br1 3.358(1) Å), and this contact could be a reason for K1 residing slightly out of the crown ether ring. The eighth coordinative bond to K1 is formed from nitro group oxygen O5′ ($1 - x$, $-0.5 + y$, $1.5 - z$) of the adjacent receptor with K1···O5′ distance of 2.774(3) Å (Figure 6b). The bromide Br1 is further hydrogen bonded with the adjacent receptor's urea group ($-1 + x$, y, z) with N1″···Br1 distance of 3.461(2) Å (N1″−H···Br1 angle 149°) and N2″···Br1 distance of 3.300(3) Å (N2″−H···Br1 angle 150°). The receptors stack along the crystallographic *b*-axis through hydrogen bonds formed between carbonyl oxygen O2′ ($1 - x$, $-0.5 + y$, $1.5 - z$) of the adjacent molecule and urea group atoms N3 and N4 [N3···O2′ distance 2.849(4) Å, N3−H···O2′ angle 156°; N4···O2′ distance 2.926(4) Å, N4−H···O2′ angle 150°; Figure 6b].

This type of solid-state structure represents a second general binding motif for receptor **R¹**, and similar structures were obtained with KI and RbCl (Figures S36 and S37).

R¹·NH₄Cl. Solid-state complex of **R¹·NH_4Cl** was obtained by slow diffusion of Et_2O into CH_3OH/DMF mixture of **R¹** with excess NH_4Cl added to the sample in aqueous stock solution.

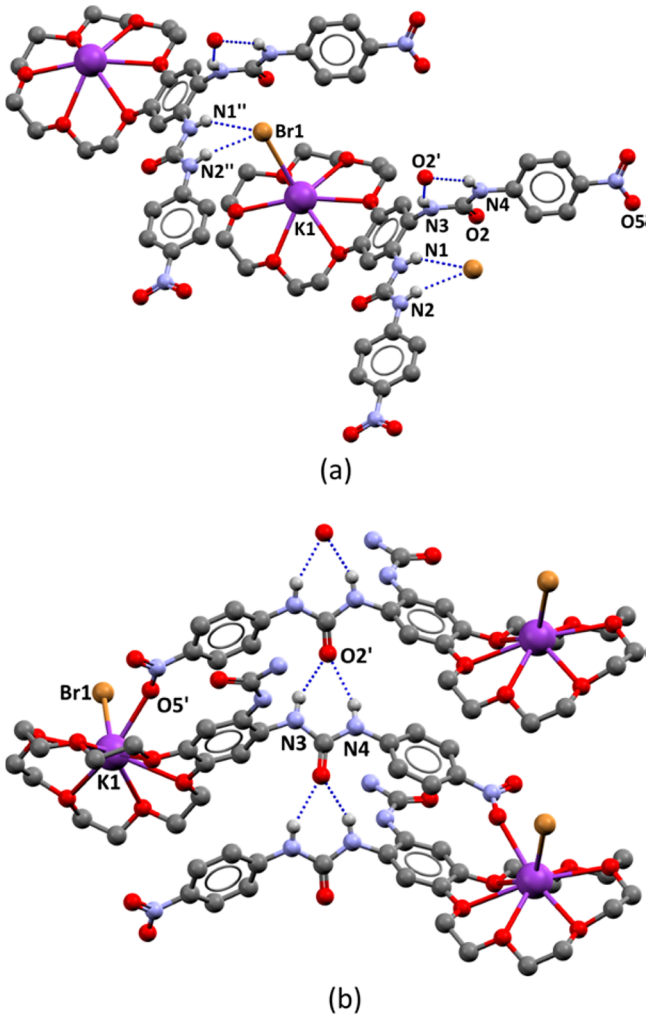

Figure 6. X-ray structure of **R¹·KBr_2**. (a) The hydrogen bonding interactions and contact ion pair formed by receptor **R¹** with KBr. Hydrogen bonds shown as dashed lines. (b) Potassium K1 has eight-coordination with crown ether oxygens, nitro oxygen O5′, and bromide Br1. Hydrogen bonds between urea nitrogens N3 and N4 and carbonyl oxygen O2′ form along the crystallographic *b*-axis. Small distortions appear in the crown ether structure and in bromide position; the distortions, nonbonding hydrogen atoms and parts of the receptor were omitted for clarity.

Addition of the guest did not result in better solubility of the receptor in CH_3OH; hence, DMF was added to the sample to dissolve the receptor. **R¹·NH_4Cl** crystallized in monoclinic space group $P2_1/c$ having a very similar structure to the **R¹·KBr_2**, **R¹·KI**, and **R¹·RbCl** complexes (Figure 7).

In **R¹·NH_4Cl** structure ammonium cation is interacting with the crown ether through three hydrogen bonds [N7···O8 distance 2.877(2) Å, N7−H···O8 angle 173°; N7···O10 distance 2.997(1) Å, N7−H···O10 angle 175°; N7···O12 distance 2.817(2) Å, N7−H···O12 angle 174°] leaving the fourth hydrogen free to form a hydrogen bond to the chloride Cl1′ ($1 + x$, y, z) with N7···Cl1′ distance of 3.277(1) Å (N7−H···Cl1′ angle 163°). The ammonium cation has also a very weak contact with nitro group oxygen O6″ ($1 - x$, $0.5 + y$, $0.5 - z$) of the adjacent molecule with N7···O6″ distance of 2.875(2) Å.

One arm of receptor **R¹** forms two hydrogen bonds to chloride Cl1 with two urea nitrogens N1 and N2 with distances

DOI: 10.1021/acs.inorgchem.5b01577
Inorg. Chem. 2015, 54, 9154−9165

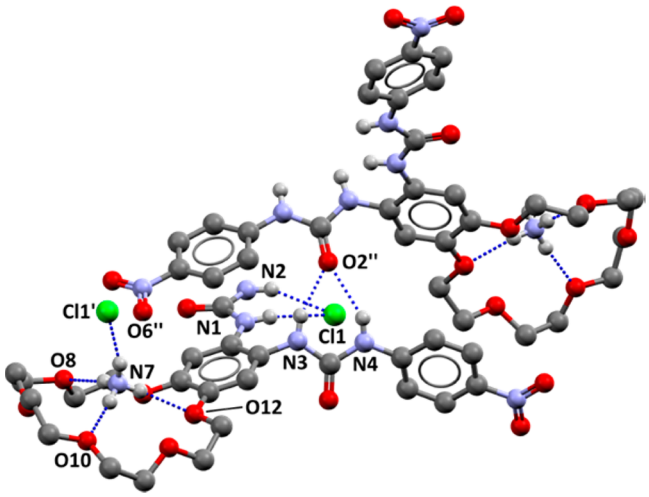

Figure 7. X-ray structure of $\mathbf{R^1{\cdot}NH_4Cl}$. Ammonium cation N7 forms a hydrogen bond aided ion pair with Cl1′. Urea nitrogens N1 and N2 hydrogen bond to chloride Cl1, while other urea group nitrogens form hydrogen bonds along crystallographic *b*-axis to carbonyl oxygen O2″ in adjacent molecule. The hydrogen bonds are shown in dashed lines. Similar structure was also obtained with NH_4Br (see Figure S38). Nonbonding hydrogen atoms and parts of the receptor were omitted for clarity.

of N1···Cl1 3.345(1) Å (N1−H···Cl1 angle 147°) and N2···Cl1 3.157(1) Å (N2−H···Cl1 angle 157°). The other arm of $\mathbf{R^1}$ forms two hydrogen bonds along the crystallographic *b*-axis by urea nitrogens N3 and N4 to the adjacent molecule's carbonyl oxygen O2″ (1 − *x*, 0.5 + *y*, 0.5 − *z*) [N3···O2″ distance 2.885(1) Å, N3−H···O2″ angle 160°; N4···O2″ distance 3.028(1) Å, N4−H···O2″ angle 150°].

Isostructural complex with NH_4Br was also obtained (see Figure S38), and in both structures the cation is residing slightly above the crown ether plane, thus being free to form a hydrogen bond aided ion pair with the anion. Contact ion pair formation seems to be more favorable to the separated cation and anion binding if the bound cation is too large for the crown ether (even if the anion is more Lewis basic) or the anion has less Lewis basic character as can be seen also with $\mathbf{R^1{\cdot}KBr\_2}$, $\mathbf{R^1{\cdot}KI}$, and $\mathbf{R^1{\cdot}RbCl}$ complexes.

***R*^{1}·*KAcO*.** Complex of $\mathbf{R^1{\cdot}KAcO}$ was crystallized by slow diffusion of Et_2O into acetone/CH_3OH solution where KAcO was added in excess in CH_3OH solution, leading to better solubility of the complex in the chosen solvent system. The complex crystallized in space group *C*2/*c* with $\mathbf{R^1}$ and 1 equiv of KAcO in the asymmetric unit forming a centrosymmetric dimer (Figure 8a,b). The structure resembles the complex obtained with KCl (Figure 5a) with a similar binding motif although the anionic guest has more complex geometry.

In the structure potassium K1 has eight-coordination residing in the middle of crown ether ring and forming six coordinative bonds to crown ether oxygens [K1···O(crown ether) distance 2.610(1)−2.994(2) Å]. Seventh coordinative bond of K1 is formed to nitro group oxygen O4′ (−*x*, *y*, 0.5 − *z*; K1···O4′ distance 2.800(2) Å) of the second molecule in the dimer. The eighth coordination site of K1 is occupied by carbonyl oxygen O2″ (0.5 − *x*, 0.5 − *y*, −*z*) of the adjacent dimer with K1···O2″ distance of 2.630(2) Å resulting in 1D coordination polymer along the crystallographic *a*-axis.

Urea nitrogens N1 and N2 form hydrogen bonds to oxygen O13 of the acetate anion [N1···O13 distance 2.971(2) Å, N1−H···O13 angle 148°; N2···O13 distance 2.706(2) Å, N2−H···O13 angle 164°; Figure 8c]. The other molecule of the dimer forms three more hydrogen bonds to acetate through urea nitrogens N3′ and N4′ with N3′ hydrogen bonding to O13 [N3′···O13 distance 2.811(2) Å, N3′−H···O13 angle 159°] and N4′ hydrogen bonding to O13 and O14 [N4′···O13 distance 3.238(2) Å, N13′−H···O13 angle 147°; N4′···O14 distance 2.964(2) Å, N4′−H···O14 angle 148°].

***R*^{1}·K_2CO_3.** Solid-state complex of $\mathbf{R^1{\cdot}K_2CO_3}$ crystallized from a mixture containing the receptor in DMF and excess KF added from aqueous stock solution. Slow evaporation of the solution resulted in red crystals (all other complexes crystallized as yellow crystals) suitable for X-ray diffraction. Carbonate anion is a result from aerial CO_2 turned into CO_3^{2-} by hydroxide generated by the basic fluoride anion in the solution, a phenomenon that has been observed previously.[33,34] The structure is formed by two receptor molecules and 1 equiv of K_2CO_3 in the asymmetric unit (Figure 9a,b). The complex resembles the dimeric structures shown previously, but in $\mathbf{R^1{\cdot}K_2CO_3}$ dimerization does not result from nitro or carbonyl oxygen's coordination with the potassium cations but through extensive hydrogen bonding interactions between $\mathbf{R^1}$ and CO_3^{2-}.

Potassium cation K1 is bound in the middle of crown ether rings with six bonds formed to crown ether oxygens [K1···OA(crown ether) 2.646(2)−2.885(2) Å]. The seventh coordination bond to K1 is formed by a water molecule O18 with K1···O18 distance 2.710(3) Å. Surprisingly, the eighth coordination site is occupied by cation-π interaction between K1 and the aromatic ring (carbons C2A′−C7A′; 2 − *x*, 1 − *y*, −*z*) in one of the arms of the molecules in the adjacent dimer with K1···centroid (C2A′−C7A′) distance of 3.219 Å (see Figure S39b). K2 also forms six coordinative bonds with crown ether having very similar bond lengths to K1 [K2···OB(crown ether) 2.666(2)−2.822(2) Å]. Two remaining coordination sites of K2 are occupied by two DMF molecules (not shown) with K2···O16 distance of 2.646(2) Å and K2···O17 distance of 2.764(2) Å.

The carbonate anion forms an extensive hydrogen bonding network with receptors A and B and water molecule O18″ with total of 13 hydrogen bonds (Figure 9c). The interactions in the anion binding resemble those seen in the structure of $\mathbf{R^1{\cdot}KAcO}$ with similar bond lengths and angles (see Supporting Information for details, Figure S39a), but clear differences between the complexes can be seen in the receptor arm conformations. For example in the structure of $\mathbf{R^1{\cdot}K_2CO_3}$ receptor A has its arms in planar conformation, and receptor B has both arms pointing toward the guest to optimize the hydrogen bonding interactions. As comparison, in the structures of $\mathbf{R^1{\cdot}KCl}$ and $\mathbf{R^1{\cdot}KAcO}$ the arms of a single receptor point in opposite directions to interact with two separate guests.

***R*^{1}·K_2SO_4.** X-ray quality crystals of complex $\mathbf{R^1{\cdot}K_2SO_4}$ were grown by slow diffusion of Et_2O into MeOH/DMF solution with excess of K_2SO_4 added in aqueous solution. The addition of the guest did not improve solubility of the receptor in methanol; thus, DMF was added to dissolve the receptor. The complex crystallized in triclinic space group $P\bar{1}$ containing a tetrameric assembly of $\mathbf{R^1}$ with 2 equiv of K_2SO_4 in the asymmetric unit (Figure 10a,b)

All the potassium cations are located in the center of the crown ethers, and each of them form six bonds with the crown ether oxygens [K1A···O(crown ether) distance 2.806(4)−

DOI: 10.1021/acs.inorgchem.5b01577
Inorg. Chem. 2015, 54, 9154−9165

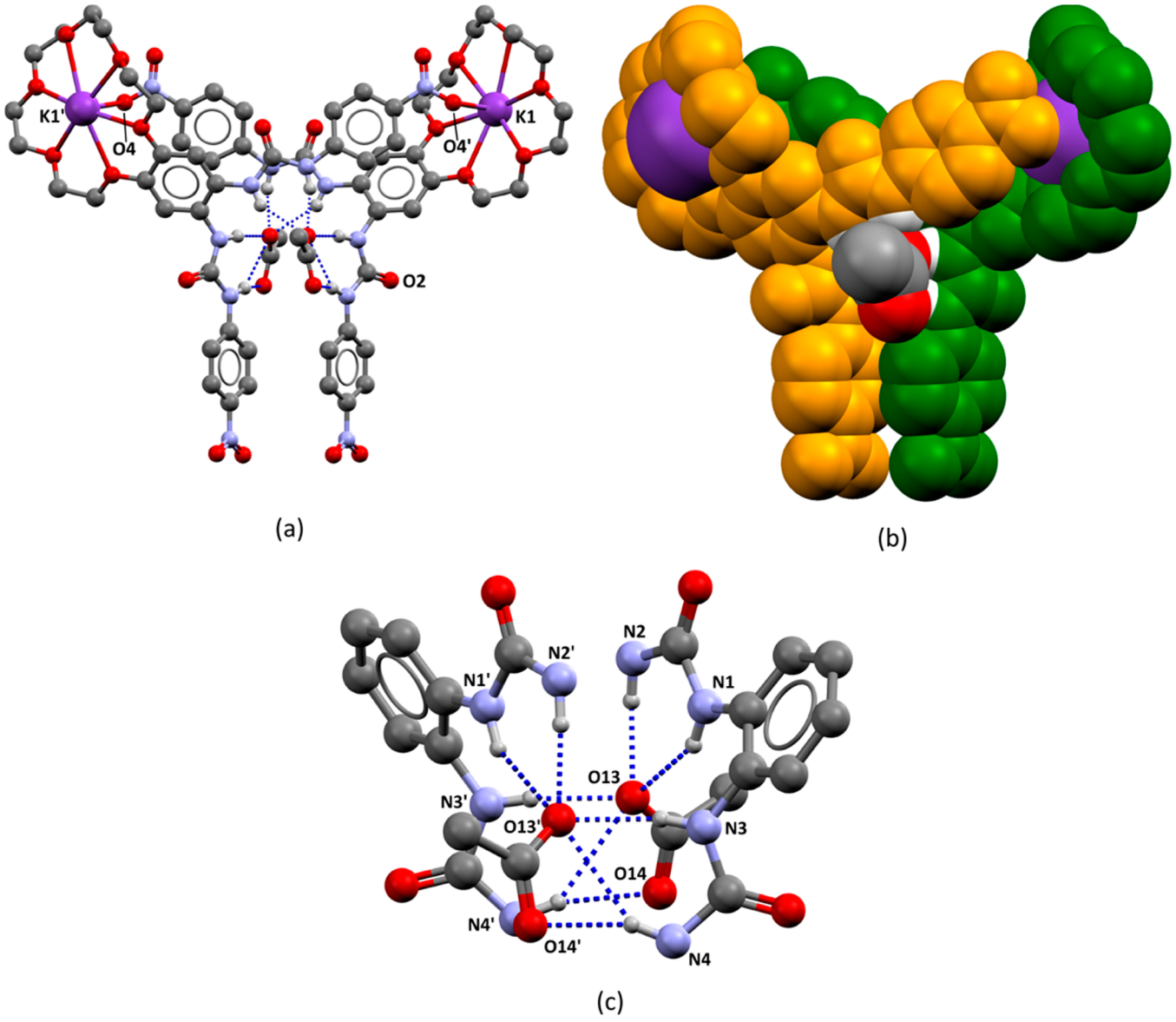

Figure 8. X-ray structure of $\mathbf{R^1}$**·KAcO**. (a) Ball-and-stick presentation of the dimer and the hydrogen bonding interactions. Hydrogen bonds are illustrated with dashed lines. (b) CPK model of the dimeric structure. (c) More detailed figure of the hydrogen bonding interactions between the dimer and two acetate anions. All nonbonding hydrogen atoms were omitted for clarity.

2.968(3) Å; K1B···O(crown ether) distance 2.78(2)−2.958(7) Å; K1C···O(crown ether) distance 2.821(5)−2.928(7) Å; K1D···O(crown ether) distance 2.713(4)−2.931(4) Å]. Potassium K1A forms seventh coordinative bond to nitro group oxygen O4B of receptor B with K1A···O4B distance of 2.874(5) Å, and K1A has two more bonds to carbonyl oxygens O1A′ and O2A′ ($2 - x$, $1 - y$, $1 - z$) in the adjacent tetramer [K1A···O1A′ distance 2.664(3) Å; K1A···O2A′ distance 2.889(4) Å]. Potassium K1C has very similar coordination environment to K1A with seventh coordinative bond formed to nitro group oxygen O5D of receptor D in the same tetramer (K1C···O5D distance 2.947(5) Å), and two more coordinative bonds are formed to carbonyl oxygens O1C″ and O2C″ ($1 - x$, $1 - y$, $-z$) in another tetramer [K1C···O1C″ distance 2.687(4) Å; K1C···O2C″ distance 2.915(6) Å]. Potassium K1B has only seven coordination with one bond formed to carbonyl oxygen O1B* ($1 - x$, $-y$, $-z$) in yet another adjacent tetramer with K1B···O1B* distance of 2.619(6) Å, and the last two coordination sites of K1D are occupied by oxygens O37 and O38 in one of the sulfate anions in the structure [K1D···O37 distance 3.076(4) Å; K1D···O38 distance 2.605(4) Å; not shown].

Tetrameric assembly of four $\mathbf{R^1}$ molecules leads to an extensive hydrogen bonding network between the four receptors and two sulfates buried inside the binding pocket covered by urea nitrogens. One sulfate ion interacts with receptors A, B, and C through nine hydrogen bonds, and the other sulfate hydrogen bonds to receptors A, C, and D with eight hydrogen bonds. The hydrogen bonding interactions resemble closely those seen with complexes $\mathbf{R^1}$**·KAcO** and $\mathbf{R^1}$**·**$\mathbf{K_2CO_3}$, and the details of the hydrogen bonding interactions are given in the Supporting Information (Figure S40). Also this structure shows different conformations of the receptors within same structure with two of the four receptors having their urea groups pointing nearly parallel to each other (Figure 10a,b; receptors A and C are yellow and green, respectively) and two

DOI: 10.1021/acs.inorgchem.5b01577
Inorg. Chem. 2015, 54, 9154−9165

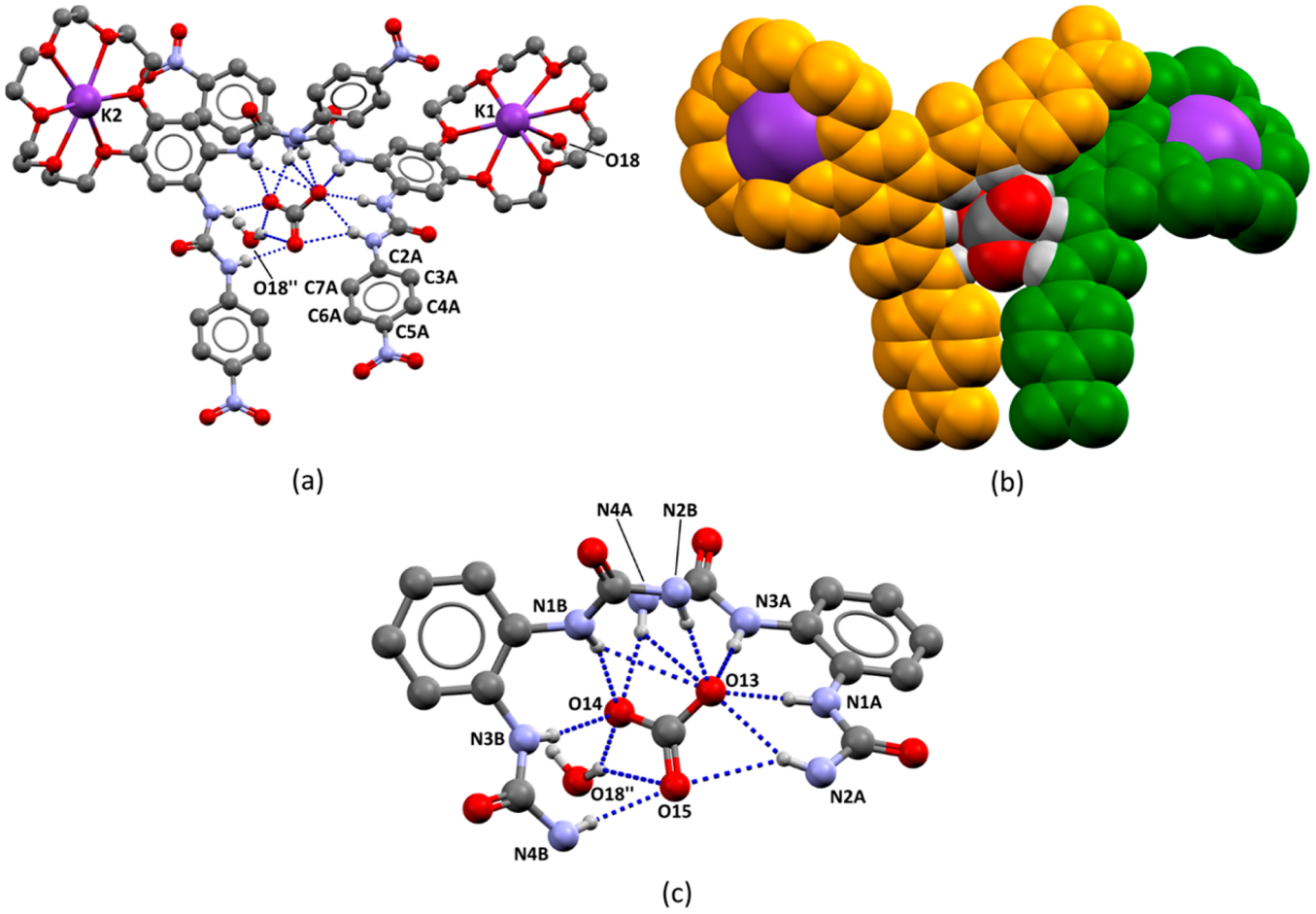

Figure 9. X-ray structure of the complex $\mathbf{R^1}\cdot K_2CO_3$. (a) Ball-and-stick presentation of the complex with two molecules of $\mathbf{R^1}$ hydrogen bonded to a carbonate anion. (b) CPK model of the asymmetric unit. (c) Hydrogen bonding interactions involved in the carbonate binding. Hydrogen bonds are shown in dashed lines. All the nonbonding hydrogen atoms, solvent molecules, and slight distortion in one crown ether are not shown for clarity.

of the urea groups pointing to opposite sides of the receptor plane and having their urea group conformations resembling those seen in the complex $\mathbf{R^1}\cdot\mathbf{KCl}$ and $\mathbf{R^1}\cdot\mathbf{KAcO}$ (receptors B and D are red and blue, respectively).

The geometry of the bound anionic guest seems to have an important effect on the receptor conformations. When $\mathbf{R^1}$ binds to a guest with more complicated geometry the receptor arms can have conformations ranging from planar to nearly parallel orientation to each other. These structures elucidate the versatility of $\mathbf{R^1}$ to have suitable conformations in the solid state for different anion geometries.

Mass Spectrometry. The complexation experiments with ESI-MS from equimolar samples showed a 2:1 complex formation between receptor $\mathbf{R^1}$ and ion pairs on positive polarization (Figure 11, Table S1). Formally the ions were observed as cation adducts $[2\mathbf{R^1}+CA+C]^+$ (C = cation, A = anion). In addition, 1:1 complexes $[\mathbf{R^1} + C]^+$ were always present in the spectra being especially abundant with ion pairs of K^+ and Na^+, which is not surprising considering the high affinity of 18-crown-6 toward these cations. Ion pair complexation of monomers was not observed, which most likely results from invisibility of $[\mathbf{R^1}+\text{ion pair}]^0$ complexes in an MS experiment. Among potassium and sodium ion pairs clearly the most abundant complex formation was observed with chlorides, which likely results from higher affinity of the urea group toward chloride anion as shown in the Solution Studies. In the case of potassium, the ion $[2\mathbf{R^1}+KCl+K]^+$ was roughly 8 times more abundant than corresponding iodide or bromide complexes. Among rubidium ion pairs, impurities originating from sodium and potassium cations interfered with the spectra, due to their higher affinity toward 18-crown-6 core, and for this reason only mixed alkali metal ions, for example, $[2\mathbf{R^1}+RbCl+Na]^+$, were observed. The 2:1 complex formation of $\mathbf{R^1}$ and ion pair was clearly a concentration-dependent process, and increasing the receptor/ion pair ratio in samples resulted in increased relative abundance of dimeric complexes and vice versa. In addition to 1:1 and 2:1 complexes, also a minor formation of assumedly sandwich-type doubly charged ions $[3\mathbf{R^1} + CA + 2C]^{2+}$ was observed (Figure 11). Ion $[2\mathbf{R^1}-H+2K]^+$ originates from cleavage of HCl from the complex suggesting that the chloride is bound through hydrogen bonding with urea functionalities in $\mathbf{R^1}$ also in gas phase.

The relative affinity of $\mathbf{R^1}$ toward different ion pairs was studied in more detail in bilateral competition experiments, in which two different ion pairs were present in the same sample in excess. The pairs used in competition experiments were chosen to uncover both the effect of cation and anion for complexation with $\mathbf{R^1}$, and the experiments were performed between KCl/KBr, KBr/KI, and KCl/NaCl (Figure 12). According to competition experiments receptor $\mathbf{R^1}$ has the highest affinity toward KCl. The comparison between cations reveals the affinity to be $K^+ \gg Na^+$, which is logical due to the

DOI: 10.1021/acs.inorgchem.5b01577
Inorg. Chem. 2015, 54, 9154−9165

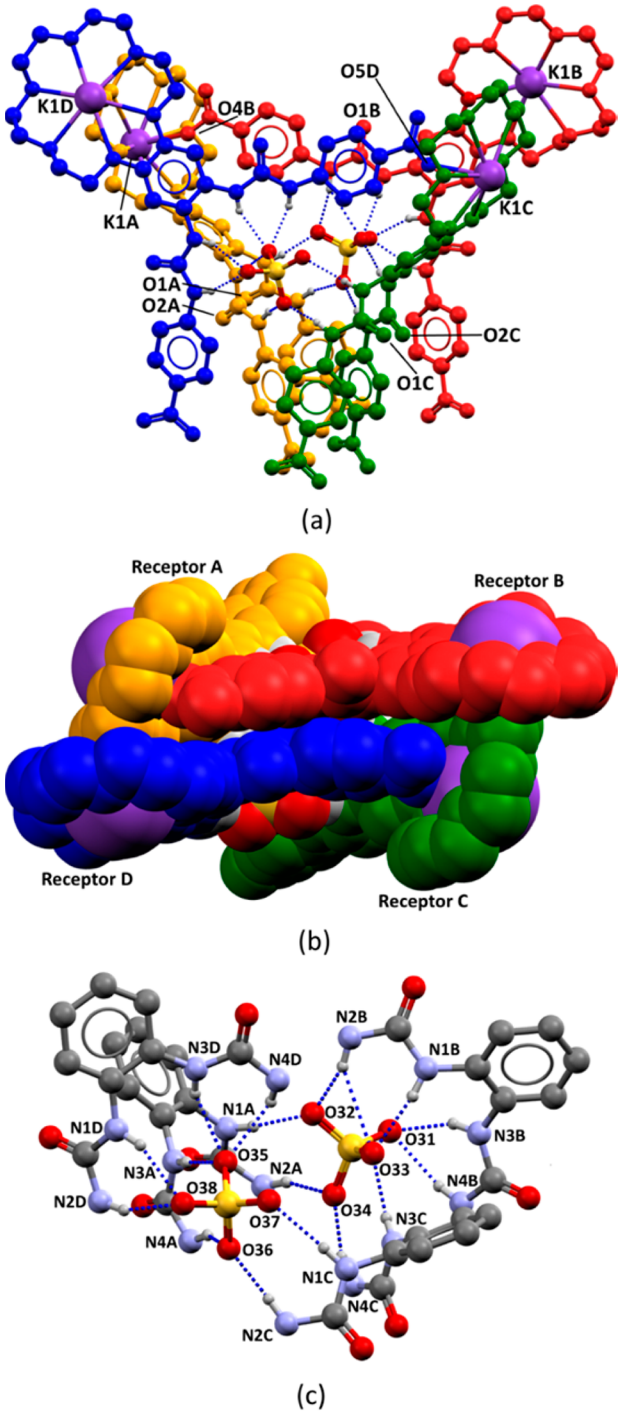

Figure 10. X-ray structure of the complex $\mathbf{R^1}\cdot K_2SO_4$. (a) Ball-and-stick presentation of the tetrameric complex (receptor A = yellow, receptor B = red, receptor C = green, receptor D = blue) with 2 equiv of K_2SO_4 present in the structure. The hydrogen bonding interactions are shown in dashed lines. (b) CPK presentations of the tetrameric complex shown from above. (c) The detailed presentations of the hydrogen bonds between the urea groups and the sulfate anions. One sulfate (oxygens O31−O34) forms nine hydrogen bonds to receptors A, B, and C, and the other sulfate (oxygens O35−O38) is hydrogen bonded to receptors A, C, and D through eight hydrogen bonds. Oxygens O37 and O38 form a coordinative bond to K1D′ in the neighboring tetrameric complex. All the nonbonding hydrogen atoms, solvent molecules, and distortion are omitted for clarity.

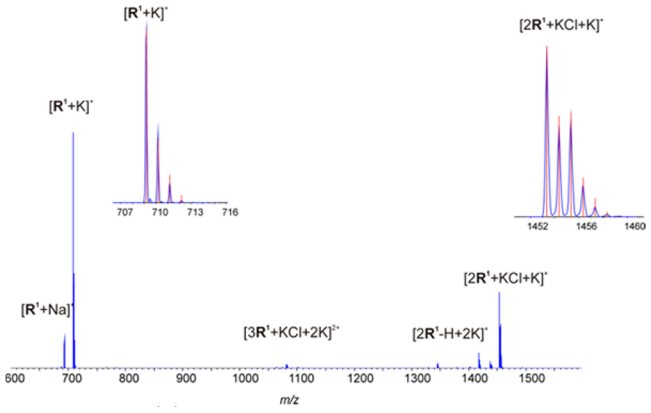

Figure 11. ESI(+)-MS spectrum measured from sample containing receptor $\mathbf{R^1}$ and KCl 1:1 (20 μM, MeOH). (insets) Fitted experimental and theoretical isotopic distributions (red solid line, calculated on the basis of natural abundances of isotopes). The $[R^1+Na]^+$ adduct ion originates from natural presence of Na^+ cations and is commonly observed in ESI-MS analysis.

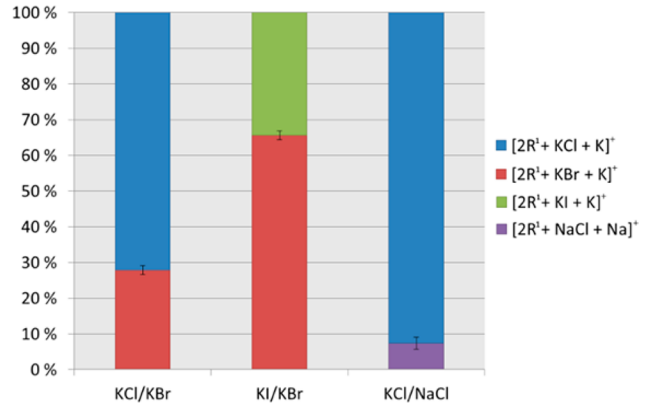

Figure 12. Relative affinity of $\mathbf{R^1}$ toward ion pairs according to ESI-MS competition experiments (molar ratio 1:1:1). Results from competing pairs KCl/KBr (left), KI/KBr (middle), and KCl/NaCl (right).

highest affinity of potassium toward 18-crown-6 scaffold. Respectively, the affinity toward anions increases in order I^- < Br^- < Cl^-, which is in accordance with the results obtained from the solution studies. Both of these effects can be rationalized by steric and Lewis basicity factors. Although solvation of anions and alkali metal cations often affects the ESI response of ions (especially when polar protic solvents are used), note that the trends observed in affinities of $\mathbf{R^1}$ are contradictory to solvation trends and can therefore be considered to originate from intrinsic properties of the receptor.

CONCLUSIONS

In summary, we have presented synthesis of a simple crown ether-based bis-urea receptor and studied its ion pair recognition characteristics in solution, solid state, and in gas phase. The detailed solution studies with cations, anions, and ion pairs has proven positive cooperativity of $[\mathbf{R^1}\cdot\text{cation}]^+$ complex toward halide anions in 4:1 $CDCl_3$/DMSO solution. This can be explained by electrostatic interactions and increased acidity of the urea protons upon cation binding leading to stronger hydrogen bonding between the receptor and the anion. All of the tested cations (Na^+, K^+, Rb^+) showed

DOI: 10.1021/acs.inorgchem.5b01577
Inorg. Chem. 2015, 54, 9154−9165

positive cooperativity with similar binding constants suggesting that the size of the cation does not play a key role in cooperativity. Comprehensive studies of the solid-state structures of the ion pair complexes, either alkali metal or ammonium cations and halide or oxyanions, give a clear picture of the structure of the binding motifs of $\mathbf{R^1}$ and the different weak interactions governing the ion pair binding. Two clearly distinguishable binding motifs were found for $\mathbf{R^1}$, yet a preference to the formation of the separated ion pair complex was observed. This is due to the stronger binding of the cation into the 18-crown-6 moiety (potassium) and its influence to the acidity of the urea protons. Then the strongly Lewis basic anions (fluoride, chloride, oxy-anions) will show enhanced binding and formation of the separated ion pair complex. When the cation is not optimally bound to the 18-crown-6 moiety (rubidium, ammonium) and the anion is a weaker Lewis base (bromide, iodide), the $\mathbf{R^1}$ prefers the contact ion pair complex. Interestingly, KBr has been found to be a watershed guest for $\mathbf{R^1}$ in solid state, and both binding motifs described above were observed in the same crystallization experiment. However, different binding motifs were not observed in solution although some of the ion pairs studied indicated 1:1 and 2:1 complex stoichiometries in solution. The mass spectrometric gas-phase studies support the solution-state studies by showing the preference for KCl binding over KBr, KI, and NaCl in the competition experiments. Investigations of oxyanion recognition and expansion of this type of crown ether bis-urea receptor family are ongoing in our laboratory.

■ ASSOCIATED CONTENT

Supporting Information

The Supporting Information is available free of charge on the ACS Publications website at DOI: 10.1021/acs.inorgchem.5b01577.

Synthesis and characterization of **2**, **3**, and $\mathbf{R^1}$, details of solution studies, Job plots, titration data and binding isotherms, details of X-ray crystallography, supporting figures of crystal structures, details of MS experiments, and MS data. (PDF)

X-ray crystallographic information of **2** (CIF)

X-ray crystallographic information of **3** (CIF)

X-ray crystallographic information of $\mathbf{R^1}$ (CIF)

X-ray crystallographic information of $\mathbf{R^1}$**·KCl** (CIF)

X-ray crystallographic information of $\mathbf{R^1}$**·KBr_1** (CIF)

X-ray crystallographic information of $\mathbf{R^1}$**·KBr_2** (CIF)

X-ray crystallographic information of $\mathbf{R^1}$**·**$\mathbf{NH_4Cl}$ (CIF)

X-ray crystallographic information of $\mathbf{R^1}$**·KAcO** (CIF)

X-ray crystallographic information of $\mathbf{R^1}$**·**$\mathbf{K_2CO_3}$ (CIF)

X-ray crystallographic information of $\mathbf{R^1}$**·**$\mathbf{K_2SO_4}$ (CIF)

X-ray crystallographic information of $\mathbf{R^1}$**·KF** (CIF)

X-ray crystallographic information of $\mathbf{R^1}$**·KI** (CIF)

X-ray crystallographic information of $\mathbf{R^1}$**·RbCl** (CIF)

X-ray crystallographic information of $\mathbf{R^1}$**·**$\mathbf{NH_4Br}$ (CIF)

■ AUTHOR INFORMATION

Corresponding Author

*E-mail: kari.t.rissanen@jyu.fi.

Notes

The authors declare no competing financial interest.

■ ACKNOWLEDGMENTS

We thank the Academy of Finland (K.R.: Project Nos. 263256 and 265328, E.K.: Nos. 284562 and 278743) and Graduate School of Univ. of Jyväskylä (T.M.) for financial support. Ms. E. Marcon and Mr. V. Holopainen are gratefully acknowledged for the help with MS measurements and synthetic work.

■ REFERENCES

(1) Steed, J. W.; Atwood, J. L. *Supramolecular Chemistry*, 2nd ed.; Wiley: Chichester, U.K., 2009.

(2) Pedersen, C. J. *J. Am. Chem. Soc.* **1967**, *89*, 7017.

(3) Pedersen, C. J. *Science* **1988**, *241*, 536.

(4) Gokel, G. W.; Leevy, W. M.; Weber, M. E. *Chem. Rev.* **2004**, *104*, 2723.

(5) Gale, P. A.; Busschaert, N.; Haynes, C. J. E.; Karagiannidis, L. E.; Kirby, I. L. *Chem. Soc. Rev.* **2014**, *43*, 205.

(6) Wenzel, M.; Hiscock, J. R.; Gale, P. A. *Chem. Soc. Rev.* **2012**, *41*, 480.

(7) Gale, P. A. *Chem. Soc. Rev.* **2010**, *39*, 3746.

(8) Caltagirone, C.; Gale, P. A. *Chem. Soc. Rev.* **2009**, *38*, 520.

(9) Gale, P. A.; Garcia-Garrido, S.; Garric, J. *Chem. Soc. Rev.* **2008**, *37*, 151.

(10) Cai, J.; Sessler, J. L. *Chem. Soc. Rev.* **2014**, *43*, 6198.

(11) Kim, S. K.; Sessler, J. L. *Acc. Chem. Res.* **2014**, *47*, 2525.

(12) Picot, S. C.; Mullaney, B. R.; Beer, P. D. *Chem. - Eur. J.* **2012**, *18*, 6230.

(13) Kim, S. K.; Sessler, J. L. *Chem. Soc. Rev.* **2010**, *39*, 3784.

(14) Kirkovits, G.; Shriver, J.; Gale, P.; Sessler, J. *J. Inclusion Phenom. Mol. Recognit. Chem.* **2001**, *41*, 69.

(15) Jones, J. W.; Gibson, H. W. *J. Am. Chem. Soc.* **2003**, *125*, 7001.

(16) Huang, F.; Jones, J. W.; Slebodnick, C.; Gibson, H. W. *J. Am. Chem. Soc.* **2003**, *125*, 14458.

(17) Huang, F.; Jones, J. W.; Gibson, H. W. *J. Org. Chem.* **2007**, *72*, 6573.

(18) Eckelmann, J.; Saggiomo, V.; Sonnichsen, F. D.; Luning, U. *New J. Chem.* **2010**, *34*, 1247.

(19) Moerkerke, S.; Le Gac, S.; Topić, F.; Rissanen, K.; Jabin, I. *Eur. J. Org. Chem.* **2013**, *2013*, 5315.

(20) Howe, E. N. W.; Bhadbhade, M.; Thordarson, P. *J. Am. Chem. Soc.* **2014**, *136*, 7505.

(21) Shukla, R.; Kida, T.; Smith, B. D. *Org. Lett.* **2000**, *2*, 3099.

(22) Barboiu, M.; Vaughan, G.; van der Lee, A. *Org. Lett.* **2003**, *5*, 3073.

(23) Barboiu, M.; Meffre, A.; Legrand, Y.-M.; Petit, E.; Marin, L.; Pinteala, M.; Lee, A. V. D. *Supramol. Chem.* **2014**, *26*, 223.

(24) Jeon, N.-J.; Yeo, H.-M.; Nam, K.-C. *Bull. Korean Chem. Soc.* **2008**, *29*, 663.

(25) Piatek, P.; Zdanowski, S.; Romanski, J. *New J. Chem.* **2015**, *39*, 2090.

(26) Sun, Z.; Pan, F.; Triyanti; Albrecht, M.; Raabe, G. *Eur. J. Org. Chem.* **2013**, *2013*, 7922.

(27) Lee, J. H.; Lee, J. H.; Choi, Y. R.; Kang, P.; Choi, M.; Jeong, K. *J. Org. Chem.* **2014**, *79*, 6403.

(28) Duggan, S. A.; Fallon, G.; Langford, S. J.; Lau, V.; Satchell, J. F.; Paddon-Row, M. *J. Org. Chem.* **2001**, *66*, 4419.

(29) Brooks, S. J.; Edwards, P. R.; Gale, P. A.; Light, M. E. *New J. Chem.* **2006**, *30*, 65.

(30) Frassineti, C.; Ghelli, S.; Gans, P.; Sabatini, A.; Moruzzi, M. S.; Vacca, A. *Anal. Biochem.* **1995**, *231*, 374.

(31) Thordarson, P. *Chem. Soc. Rev.* **2011**, *40*, 1305.

(32) Shukla, R.; Kida, T.; Smith, B. D. *Org. Lett.* **2000**, *2*, 3099.

(33) Custelcean, R.; Delmau, L. H.; Moyer, B. A.; Sessler, J. L.; Cho, W.; Gross, D.; Bates, G. W.; Brooks, S. J.; Light, M. E.; Gale, P. A. *Angew. Chem., Int. Ed.* **2005**, *44*, 2537.

(34) Ravikumar, I.; Ghosh, P. *Chem. Commun.* **2010**, *46*, 1082.

DOI: 10.1021/acs.inorgchem.5b01577
Inorg. Chem. 2015, 54, 9154−9165